

# Photorefractive behavior of Ba[Fe(CN)<sub>5</sub>NO]·3H<sub>2</sub>O in the red and near-infrared spectral range

Th. Woike, M. Imlau, and S. Haussühl

*Institut für Kristallographie, Universität zu Köln, Zùlpicher Strasse 49b, D-50674 Köln, Germany*

R. A. Rupp

*Institut für Experimentalphysik, Universität Wien, Boltzmannstrasse 5, A-1090 Wien, Austria*

R. Schieder

*I. Physikalisches Institut, Universität zu Köln, Zùlpicher Strasse 77, D-50937 Köln, Germany*

(Received 3 February 1998)

Phase gratings can be written in acentric Ba[Fe(CN)<sub>5</sub>NO]·3H<sub>2</sub>O single crystals on the basis of extremely long-living metastable electronic states at temperatures below  $T=213$  K after preexposure with light in the range of 350–580 nm. The modulation of the refractive index reaches values up to  $\Delta n=5.3\times 10^{-4}$  in the red and  $\Delta n=1.6\times 10^{-4}$  in the near-infrared spectral range. Beam-coupling experiments show that there is no phase shift between the light interference pattern and the resulting refractive index grating. The dynamical behavior of the diffraction efficiency during the writing process depends on the depopulation velocity of the metastable electronic states SI and SII and on the transfer velocity from SI into SII. The maximum efficiency of  $\eta=72\%$  is reached at an exposure of  $Q=27$  J/cm<sup>2</sup> with  $\lambda=632.8$  nm. The grating is stable against irradiation with light of wavelength  $\lambda=1047$  nm and cannot be destroyed with an exposure of up to  $Q=600$  J/cm<sup>2</sup>. In comparison to centrosymmetric Na<sub>2</sub>[Fe(CN)<sub>5</sub>NO]·2H<sub>2</sub>O, where the refractive index cannot be modulated perpendicularly to the mirror plane  $m$ , such a restriction does not exist in the acentric single crystal. [S0163-1829(98)05437-X]

## INTRODUCTION

Two-wave and four-wave mixing are extensively used to characterize optical properties of photorefractive or photochromic materials. These techniques are especially suited for the study of holographic gratings formed by excitation of metastable states as shown for the transition-metal ions Cr<sup>3+</sup> and Mn<sup>2+</sup> (Refs. 1,2) and in the case of Fe(II) spin-crossover systems.<sup>3</sup> From the diffracted intensity the polarizabilities of Cr<sup>3+</sup> in the excited states could be determined and the refractive index change of  $\Delta n=5\times 10^{-5}$  found in spin-crossover compounds was explained by an increase of the metal-ligand bondlength. Recently we proved the existence of refractive-index and absorption gratings in Na<sub>2</sub>[Fe(CN)<sub>5</sub>NO]·2H<sub>2</sub>O (Sodium nitroprusside, NaNP) single crystals by two-wave mixing experiments.<sup>4</sup> They originate from the excitation of extremely long-lived metastable electronic states. Population of these states can be performed in anions with empty low-lying antibonding  $\Pi^*(\text{NO})$  orbitals, e.g.,  $[ML_5\text{NO}]^{2-}$ , whereby  $M=\text{Fe, Ru, or Os}$  and  $L=\text{ligand}$ .<sup>5,6</sup> Hence the photorefractive effect does not require the presence of additional dopants or defects. The modulation of the refractive index  $\Delta n$  or of the absorption coefficient  $\Delta\alpha$  are related to the population and can therefore be adjusted by irradiation, since the population of the new states depends on light exposure  $Q=I\cdot t$ , i.e., the product of light intensity  $I$  and exposure time  $t$ . The wavelength dependences of  $\Delta n$  and  $\Delta\alpha$  are determined by the dispersion behavior of the metastable states, which can be varied by changing the central atom  $M$  or the ligand  $L$ . In NaNP holographic gratings can be generated in the visible and near-infrared spectral range. The refractive index change  $\Delta n$  is

modulated by more than  $2\times 10^{-3}$ . In the  $[\text{Fe}(\text{CN})_5\text{NO}]^{2-}$  anion two metastable states SI and SII can be populated with light in the spectral range of 350–580 nm below temperatures of 200 K (SI) and 150 K (SII), respectively. They can be reversibly transferred to the ground state (GS) by irradiation with light in the spectral range of 600–1200 nm or by heating above 200 K. A population transfer from SI into SII is possible in the spectral range of 900–1200 nm. Therefore, there are at least three ways for the generation of holographic gratings: In the write mode by population of SI or SII (GS→SI,SII) and in the erase mode after homogeneous population either by transfer (SI→SII) or by deexcitation of SI or SII (SI,SII→GS).

In this paper, we report about the photorefractive and photochromic behavior of Ba[Fe(CN)<sub>5</sub>NO]·3H<sub>2</sub>O (Barium nitroprusside, BaNP) in the red and near-infrared spectral region. While NaNP belongs to the centrosymmetric space group  $Pn\bar{m}$ , BaNP undergoes a phase transition at  $T=233$  K from the space group  $Pbcm$  into  $Pca2_1$ ,<sup>7</sup> so that we can analyze the behavior of metastable states in holographic experiments for a point-symmetry group differing from the one of NaNP.

## EXPERIMENTAL DETAILS

### Sample preparation and structural details

Single crystals of BaNP of optical quality and dimensions up to  $90\times 40\times 40$  mm<sup>3</sup> were grown from aqueous solutions by controlled evaporation and cooling between 311 and 306 K. The growth velocity was kept below 2 mm per day. The orthorhombic crystals (space group  $Pbcm$ ,  $Z=4$ ) develop to

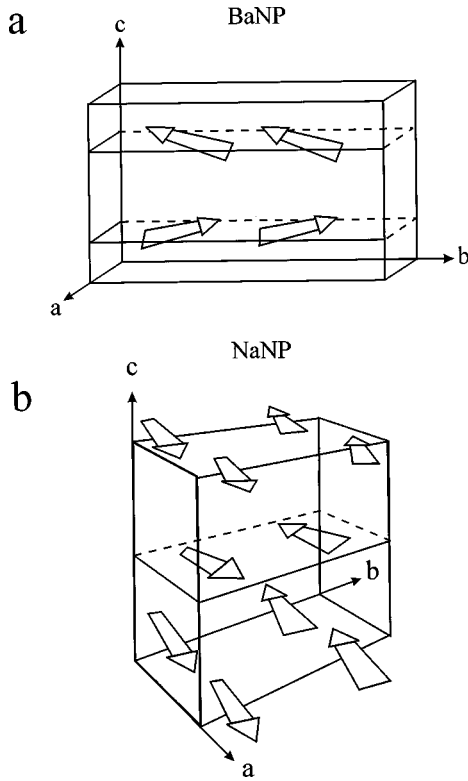


FIG. 1. The direction of the N-C-Fe-N-O axis of the  $[\text{Fe}(\text{CN})_5\text{NO}]^{2-}$  anions are indicated by arrows (a) in BaNP below  $T=233$  K inclined by  $6.5^\circ$  and  $13^\circ$  with respect to the  $b$  and  $c$  axis, respectively, (b) in the  $a$ - $b$  mirror plane of NaNP.

pinacoids  $\{100\}$  and  $\{010\}$ , prism  $\{120\}$  and dipyrmaid  $\{111\}$ . Structural details are given in Ref. 8. Below 300 K the acentric modification  $\text{Ba}[\text{Fe}(\text{CN})_5\text{NO}] \cdot 6.5\text{H}_2\text{O}$  (space group  $Cmc2_1$ ,  $Z=8$ ) grows in the monodomain structure,<sup>9</sup> which is not considered here. Crystal plates were cut from large single crystals, ground to the desired thickness of 0.2–0.5 mm and finally polished with  $\text{Cr}_2\text{O}_3$  powder. The excellent cleavage perpendicular to the  $b$  axis impedes the preparation of thin polished plates with other orientations than (010). Holographic measurements are restricted by this condition.

The quasifourfold N-C-Fe-N-O axes are symbolized in Figs. 1(a) and 1(b) by arrows within the unit cell of BaNP [Fig. 1(a)] and NaNP [Fig. 1(b)]. In the acentric phase of BaNP below  $T=233$  K these axes are orientated at angles of  $6.5^\circ$  and  $13^\circ$  with respect to the  $c$  and  $b$  axis, respectively, so that no mirror plane exists. Because of the phase transition we cannot decide whether the single crystal is in a multi- or single domain state. Apart from a negligible deviation of approximately  $3^\circ$  the Fe-N-O chain forms a straight line. If the electric-field vector  $\mathbf{E}$  of the incident beams is orientated along one of the crystallographic axes, then there are always components along this quasifourfold axis for BaNP. Since in NaNP the anions are lying within the  $a$ - $b$  mirror plane at an angle of  $\pm 35.8^\circ$  with respect to the  $a$  axis, the electric field vibrates exactly perpendicularly to the quasifourfold axis for  $\mathbf{E} \parallel c$ .

#### Metastable states

The maximum population of the metastable states SI and SII depends on the wavelength and light polarization. For

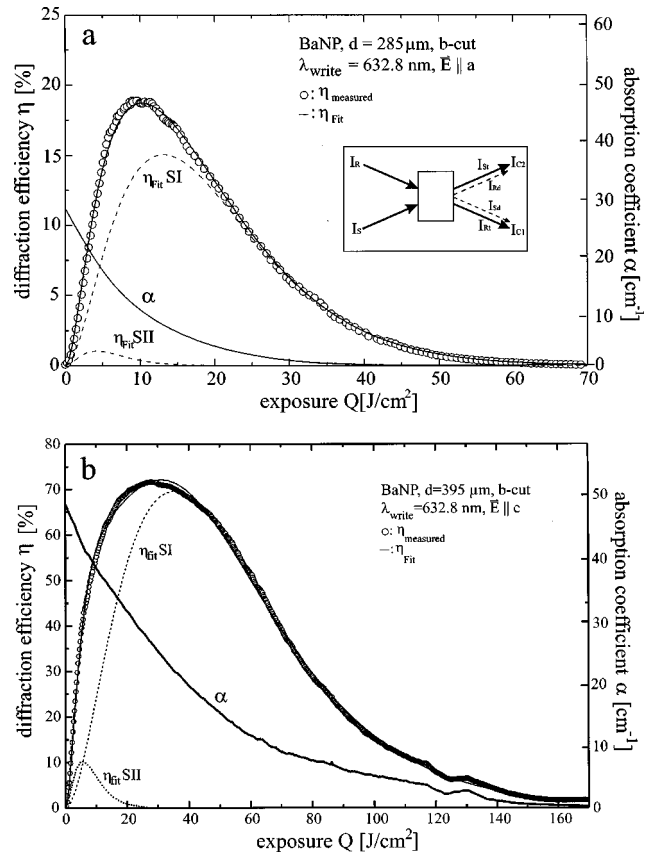


FIG. 2. Diffraction efficiency  $\eta$  and absorption coefficient  $\alpha$  of a BaNP ( $b$  cut) single crystal versus exposure. Gratings are written in the erase mode at wavelength  $\lambda=632.8$  nm after preexposure with  $\lambda=476.5$  nm,  $\mathbf{E} \parallel c$ . (a) Preexposure:  $Q=485$   $\text{J}/\text{cm}^2$ , crystal thickness  $285$   $\mu\text{m}$ , read out with polarization parallel to the crystallographic  $a$  axis. (b) Preexposure:  $Q=856$   $\text{J}/\text{cm}^2$ , crystal thickness  $395$   $\mu\text{m}$ , read out with polarization parallel to the crystallographic  $c$  axis.

$\lambda=(450 \pm 20)$  nm 30% of the anions of BaNP can be transferred into SI and about 1% into SII with  $\mathbf{E} \parallel a$  or  $c$  axis. Choosing  $\mathbf{E} \parallel b$  axis and  $\lambda=(450 \pm 20)$  nm the populations are 4% (SI) and 0.7% (SII). After preexposure in the blue-green spectral range, irradiation with  $\lambda=1064$  or  $1047$  nm and  $\mathbf{E} \parallel a$  or  $c$  axis transfers about 2/3 of the anions from SI into SII and 1/3 into GS. The decay temperatures of both states are 213 K (SI) and 145 K (SII), i.e., substitution of Na by Ba increases the decay temperature of SI by 13 K.

#### Experimental setup

Holographic investigations are performed by writing and analyzing elementary holographic gratings in BaNP single crystals. Details of the experimental arrangement are given in Ref. 4. During illumination of the samples with a sinusoidally modulated light interference pattern, the transmitted and diffracted intensities are measured by alternatively closing one of the incident beams. The diffraction efficiency  $\eta$  is defined following the designations of the inset in Fig. 2(a) as  $\eta_R = I_{Rd} / (I_{Rt} + I_{Rd})$  and  $\eta_S = I_{Sd} / (I_{St} + I_{Sd})$ , whereby  $I_{Rt}$ ,  $I_{St}$  and  $I_{Rd}$ ,  $I_{Sd}$  are the transmitted and diffracted intensities of the incoming waves  $R$  and  $S$  with the intensities  $I_R$  and  $I_S$ , respectively. The ratio of the incoming beams is

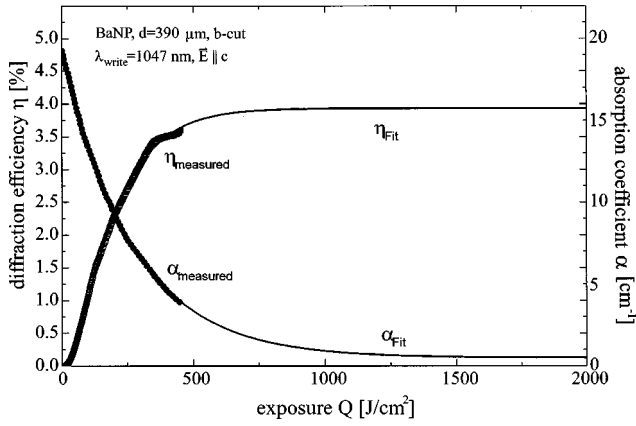


FIG. 3. Diffraction efficiency  $\eta$  and absorption coefficient  $\alpha$  of a BaNP (*b* cut) single crystal in dependence on the exposure. Gratings are written in the erase mode with  $\lambda=1047$  nm, polarization parallel to the crystallographic *c* axis, after preexposure of  $Q=644$  J/cm<sup>2</sup> with  $\lambda=476.5$  nm and polarization parallel to the crystallographic *a* axis.

adjusted to  $I_R/I_S=1$ , so that the degree of modulation gives  $m=(2\sqrt{I_R \cdot I_S})/(I_R+I_S)=1$ . For beam-coupling analysis the phase between the incoming beams is shifted after the writing process by a mirror mounted on a piezoelectric element and the transmitted intensities  $I_{C1}$  and  $I_{C2}$  are measured as a function of the external phase shift  $\phi_{\text{ext}}$ . All measurements were performed at the temperature  $T=90$  K in the erase mode with a HeNe laser ( $\lambda=632.8$  nm) and a Nd-YLF laser ( $\lambda=1047$  nm). The light intensities  $I_R=I_S=I_0$  were 23.8 mW/cm<sup>2</sup> at 632.8 nm and 31 mW/cm<sup>2</sup> at 1047 nm. Preexposure of all samples was realized by homogeneous irradiation with light of an Ar<sup>+</sup> laser ( $\lambda=476.5$  nm). All gratings were written at a Bragg angle of  $\theta=7^\circ$  corresponding to spacings of the gratings of  $\Lambda=2.60$   $\mu\text{m}$  (632.8 nm) and  $\Lambda=4.30$   $\mu\text{m}$  (1047 nm). The measured parameters are given as a function of the exposure  $Q=I \cdot t$ , since the velocity and the degree of population of the metastable states SI and SII depend on  $Q$ .

## EXPERIMENTAL RESULTS

### Efficiency

Figures 2(a) and 2(b) show the diffraction efficiencies  $\eta_R$  and  $\eta_S$  measured as a function of the exposure  $Q$  for an elementary holographic grating written in the erase mode at a wavelength  $\lambda=632.8$  nm. The polarizations of the incoming beams for both, writing and readout processes, were oriented parallel to the crystallographic *a* axis [Fig. 2(a)] and crystallographic *c* axis [Fig. 2(b)]. The measurements show nearly identical dynamic behavior for the diffraction efficiencies  $\eta_R$  and  $\eta_S$  and a maximum value of about 19% for  $\mathbf{E}\parallel a$  axis at  $Q=10$  J/cm<sup>2</sup> and 72% for  $\mathbf{E}\parallel c$  axis at  $Q=27$  J/cm<sup>2</sup>. A decrease to zero is observed for an exposure larger than  $Q=200$  J/cm<sup>2</sup>,  $\mathbf{E}\parallel c$  axes, and for  $Q=60$  J/cm<sup>2</sup>,  $\mathbf{E}\parallel a$  axes, respectively. Assuming that the grating is a pure phase grating and that its thickness is equal to the thickness of the sample, a point to be discussed below, the amplitude  $\Delta n$  of the refractive index can be calculated from Kogelnik's formula for pure phase gratings.<sup>10</sup> In the maximum  $\Delta n$  reaches  $5.3 \times 10^{-4}$  ( $\mathbf{E}\parallel c$ ) and  $3.2 \times 10^{-4}$  ( $\mathbf{E}\parallel a$ ), respectively. Fig-

ure 3 shows the development of the diffraction efficiency measured in the near-infrared spectral range at  $\lambda=1047$  nm in the erase mode for  $\mathbf{E}\parallel c$ . We find that again  $\eta_R$  and  $\eta_S$  are equal. The maximum value of  $\eta=4\%$  corresponds to a modulation of the refractive index of  $\Delta n=1.6 \times 10^{-4}$ . Contrary to the measurements in the red spectral range we could not detect a decrease of  $\eta$  with an exposure up to 600 J/cm<sup>2</sup>.

In the ground state the absorption coefficient at  $\lambda=632.8$  nm is  $\alpha(Q=0)=0.1$  cm<sup>-1</sup>. From the measured transmitted and diffracted intensities we can determine the behavior of the absorption coefficient  $\alpha(Q)$  using  $I_{Rt}+I_{Rd}=I(Q)=I_0 \exp(-\alpha(Q) \cdot d)$  and  $I_{St}+I_{Sd}=I(Q)=I_0 \exp(-\alpha(Q) \cdot d)$ , respectively, with  $I_0=I_R+I_S$ . In Figs. 2(a) and 2(b) the decrease of  $\alpha$  is shown in dependence of the exposure  $Q$ . The changes in Figs. 2(a) and 2(b) reflect the depopulations of the metastable states.

The same situation is given in Fig. 3, in which  $\alpha$  decreases from 20 to 0.1 cm<sup>-1</sup> due to the transfer SI→SII. This shows that the absorption band of SI disappears by the transfer, and that the crystal becomes transparent in the near-infrared spectral range. As the new absorption band of SII is lying in the visible spectral region its behavior cannot be detected with the used wavelengths. Starting with a population of 12% for SI and of 1% for SII we get 9% for SII at  $Q=400$  J/cm<sup>2</sup>, since about 1/3 of the anions in SI are transferred into GS and 2/3 into SII by irradiation with  $\lambda=1047$  nm.

In Figs. 2(a) and 2(b) the measured efficiencies are fitted with Kogelnik's formula  $\eta=\sin^2(\pi \Delta n d)/(\lambda \cos \theta)$  for pure phase gratings, assuming that the refractive index modulation increases by  $[1-\exp(-Q/Q_1^{\text{SI}})]$  and  $[1-\exp(-Q/Q_1^{\text{SII}})]$  and decreases by  $[\exp(-Q/Q_2^{\text{SI}})]$  and  $[\exp(-Q/Q_2^{\text{SII}})]$  for SI and SII, respectively. In a first approximation we suggest, that the change of the refractive index is proportional to the population of the metastable electronic states, so that the growth and decay functions are weighted by the starting values of the populations  $P_I$  and  $P_{II}$ .  $\Delta n(Q)$  is then given by

$$\Delta n(Q) = P_I(1 - e^{-Q/Q_1^{\text{SI}}})e^{-Q/Q_2^{\text{SI}}} + P_{II}(1 - e^{-Q/Q_1^{\text{SII}}})e^{-Q/Q_2^{\text{SII}}}. \quad (1)$$

The small amount of SII is visible in both measurements, where a maximum of  $\eta=10\%$  is found at  $Q=5$  J/cm<sup>2</sup>. This is in good accordance with the low population of SII. Without the contribution of SII the spectra could not be fitted with sufficient accuracy. SII is completely destroyed at about  $Q=25$  J/cm<sup>2</sup> for  $\mathbf{E}\parallel c$  and at about  $Q=15$  J/cm<sup>2</sup> for  $\mathbf{E}\parallel a$  axis.

The fit parameters for SII are

$$\mathbf{E}\parallel c, \quad Q_1^{\text{SII}}=18.6 \text{ J/cm}^2, \quad Q_2^{\text{SII}}=7.0 \text{ J/cm}^2,$$

$$\mathbf{E}\parallel a, \quad Q_1^{\text{SII}}=19.6 \text{ J/cm}^2, \quad Q_2^{\text{SII}}=5.0 \text{ J/cm}^2.$$

The fit parameters for SI are

$$\mathbf{E}\parallel c, \quad Q_1^{\text{SI}}=52.1 \text{ J/cm}^2, \quad Q_2^{\text{SI}}=50.0 \text{ J/cm}^2,$$

$$\mathbf{E}\parallel a, \quad Q_1^{\text{SI}}=99.1 \text{ J/cm}^2, \quad Q_2^{\text{SI}}=14.0 \text{ J/cm}^2.$$

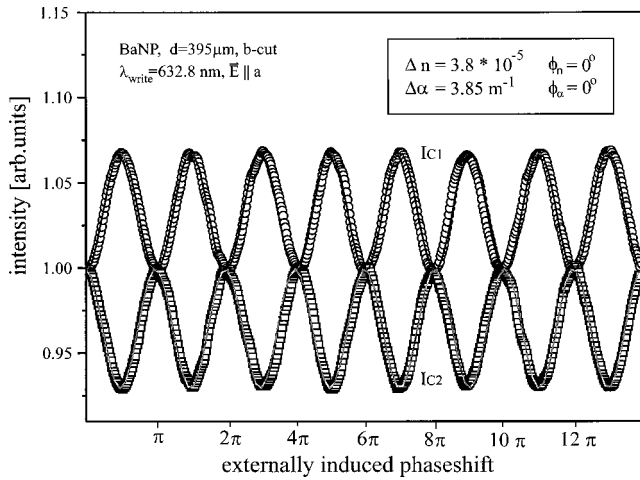


FIG. 4. Beam-coupling analysis with an externally induced phase shift  $\phi_{\text{ext}}$ . The coupled intensities  $I_{C1}$  and  $I_{C2}$  are measured at  $\lambda=632.8$  nm with polarization parallel to the  $c$  axis in a  $b$  cut of BaNP with a preexposure of  $Q=900$  J/cm<sup>2</sup> at  $\lambda=476.5$  nm. Crystal thickness:  $d=395$   $\mu\text{m}$ .

They specify the exposure which is needed to reach the  $e^{-1}$  value of the diffraction efficiencies. However, the revealed ratios for the populations,  $P_I/P_{II}=1.2$  for readout polarization parallel  $c$  axis and  $P_I/P_{II}=6.3$  parallel  $a$  axis, indicate a more complex dependence of the refractive index on the population, which has to be analyzed in further experiments.

The formation of the grating by the transfer SI→SII (Fig. 3) can be fitted with the single-exponential expression  $[1 - \exp(-Q/Q_1^{\text{SII}})]$  resulting in  $Q_1^{\text{SII}}=138.0$  J/cm<sup>2</sup>. The saturation value of  $\eta=4\%$  corresponds with the maximum of SII in Fig. 2, considering the different preexposures and the condition that only about 2/3 of SI is transferred into SII.

### Beam-coupling analysis

Beam-coupling experiments reveal the contribution of refractive-index and absorption gratings to the diffraction efficiency  $\eta$  and the possible phase shifts between the interference pattern and the gratings in the crystal. In Fig. 4 the experimental results of the beam-coupling experiments are shown for a grating written in the erase mode at  $\lambda=632.8$  nm and for polarization  $\mathbf{E}\parallel c$  after preexposure of  $Q=125$  J/cm<sup>2</sup> with  $\lambda=476.5$  nm,  $\mathbf{E}\parallel c$ . The transmitted intensities  $I_{C1}$  and  $I_{C2}$  are plotted versus the externally induced phase shift  $\phi_{\text{ext}}$ . Both intensities show a sinusoidal behavior. Evaluating this spectrum according to the procedure of Kahmann,<sup>11</sup> which is in principle a Fourier analysis of the measured data, we obtain the following results: the modulation of the refractive index is given by  $\Delta n=3.8\times 10^{-5}$ , the modulation of the absorption coefficient by  $\Delta\alpha=3.85$  m<sup>-1</sup>, the phase shift of the refractive-index grating with respect to the incoming light interference pattern by  $\phi_n=0^\circ$ , and that of the absorption grating by  $\phi_\alpha=0^\circ$  and the ratio of the incoming beams by  $I_R/I_S=1$ . In comparison to the results of the diffraction efficiency the light-induced modulation of the refractive index is about one order of magnitude smaller because of the lower preexposure [ $Q=125$  J/cm<sup>2</sup>].

### DISCUSSION

Elementary holographic gratings can be written with large diffraction efficiencies in the erase mode. The fact that these efficiencies may exceed 70% [Fig. 2(b)] and the results of the beam-coupling experiments prove that phase gratings are dominant. This identifies BaNP as the second single-crystalline material with the property that phase gratings can be written by excitation of metastable electronic states. The domain structure of BaNP in the acentric point group  $Pca2_1$  has no influence on the photorefractive behavior. A poling procedure is not necessary. The diffraction efficiencies  $\eta_R$  and  $\eta_S$  are equal, so that the Borrmann effect<sup>12</sup> can be excluded. In contrast to NaNP we observe a modulation of the refractive index in BaNP for  $\mathbf{E}\parallel c$  axis. In this special condition of NaNP as shown in Fig. 1(b), the N-C-Fe-N-O axis lies in the  $a$ - $b$  mirror plane, and with  $\mathbf{E}\parallel c$  axis (perpendicular to the mirror plane) no modulation of the refractive index can be observed. However, gratings can be detected with a probe beam polarized along the  $a$  or  $b$  axis, so that gratings are written with  $\mathbf{E}\parallel c$  axis but cannot be the readout with  $\mathbf{E}\parallel c$  axis.

In BaNP there is no restriction because there is no mirror plane. Phase gratings can be written and detected with polarization along all three crystallographic axes. Since the angle between the N-C-Fe-N-O axis and the crystallographic axes is very small, only the loss of the mirror plane can be responsible for this behavior. The direction of the grating vector  $\mathbf{K}$ ,  $|\mathbf{K}|=4\pi\sin\theta/\lambda$ , is not important for the writing of holographic gratings, as we measured equal diffraction efficiencies for  $\mathbf{K}\parallel a$  and  $\mathbf{K}\parallel c$  at the same polarization of the writing beams  $\mathbf{E}\parallel a$  and  $\mathbf{E}\parallel c$  for each direction of  $\mathbf{K}$ .

The different behavior of the diffraction efficiency in the red and infrared spectral range can be explained by the depopulation of SI and SII ( $\lambda=632.8$  nm) and the transfer SI→SII ( $\lambda=1047$  nm): In the red spectral range both SI and SII are exponentially depopulated by irradiation into the ground state, but with different depopulation velocities. Therefore, two independent modulations of the refractive index are built up with exposure, leading to the total measured diffraction efficiency. Irradiation with light in the near-infrared spectral range results in a transfer of about 1/3 of SI into GS and 2/3 into SII. In BaNP we could not find a depopulation of SII with an exposure up to  $Q=600$  J/cm<sup>2</sup>, so that SII is responsible for the holographic gratings. In the beginning of the writing process in the red spectral range the modulation of the refractive index results by the decrease of SII. The fit for both polarizations [Figs. 2(a) and 2(b)] shows, that with increasing exposure the main contribution for the diffraction efficiency is made by SI. In the infrared spectral range only SII is responsible for the build up of a modulation of the refractive index leading to a low value of the refractive index up to  $\Delta n=1.6\times 10^{-4}$ . This result is in accordance with the measurements at  $\lambda=632.8$  nm, where also low amounts of diffraction efficiencies result by the depopulation of SII. In both cases the absorption coefficient  $\alpha(Q)$  decreases exponentially to  $\alpha=0.1$  cm<sup>-1</sup> due to the complete depopulation of SI. Since  $\alpha(Q)=N(Q)\sigma(\lambda)$  is given by the product of the density  $N(Q)$  of the anions and the cross section  $\sigma(\lambda)$ , we detect at  $\lambda=632.8$  nm only the disappearance of  $N$  in the metastable state SI until GS is reached,

which explains the erasure of the phase grating. At  $\lambda=1047$  nm  $\alpha(Q)$  also approaches exponentially  $\alpha=0.1$  cm<sup>-1</sup> due to the complete depopulation of SI, but this behavior shows that the absorption band of SII lies in the visible spectral range and that BaNP is completely transparent at  $\lambda=1047$  nm, so that only phase gratings exist. The small residual value of  $\alpha=0.1$  cm<sup>-1</sup> in GS, measured by absorption spectroscopy, is a result of inhomogeneities of the crystal surface produced during the polishing procedure. The probe light is scattered and therefore an extinction is measured additionally to the material absorption.

From the fact that the phase grating is unshifted with respect to the intensity pattern, we conclude that the photorefractive effect is a local response of the light modulation and most probably results from the local excitation of  $[\text{Fe}(\text{CN})_5\text{NO}]^{2-}$  anions, but not by the conventional electrooptical effect. No migration of charge carriers by diffusion or drift and no photovoltaic effect could be detected so far. Considering in a rough approximation the Lorenz-Lorentz

formula  $N \cdot p = 3(n^2 - 1/n^2 + 1)$ , whereby  $N$  is the concentration and  $p$  the polarizability of the anions, the reason for the modulation of the refractive index can be found in the differing electronic polarizability  $p^{\text{SI}}$  and  $p^{\text{SII}}$  of the anions and the change of the densities  $N^{\text{SI}}$ ,  $N^{\text{SII}}$  of the metastable states SI and SII and the analog quantities in the ground state. The consequence of the local photorefractive effect is that the signal wave is not amplified by two wave mixing, and therefore, the high diffraction efficiencies result from the large light-induced modulation of the refractive index. Because of the electronic nature of the photorefractive effect no dark decay of the gratings exists if the temperature is sufficiently below the decay temperatures of the electronic states.

#### ACKNOWLEDGMENTS

This work was supported by the Deutsche Forschungsgemeinschaft Wo 618/1-2 and SFB 225, project A6. Th. Woike is very indebted to the SFB 225 for his stay in Osnabrück.

<sup>1</sup>S. C. Weaver and St. A. Payne, Phys. Rev. B **40**, 10 727 (1989).

<sup>2</sup>A. Suchocki, Z. Kalinski, J. M. Langer, and R. C. Powell, J. Appl. Phys. **71**, 28 (1992).

<sup>3</sup>A. Hauser, Chem. Phys. Lett. **202**, 173 (1993).

<sup>4</sup>Th. Woike, S. Haussühl, B. Sugg, R. A. Rupp, J. Beckers, M. Imlau, and R. Schieder, Appl. Phys. B: Lasers Opt. **63**, 243 (1996).

<sup>5</sup>Th. Woike and S. Haussühl, Solid State Commun. **86**, 333 (1993).

<sup>6</sup>K. Ookubo, Y. Morioka, H. Tomizawa, and E. Miki, J. Mol. Struct. **379**, 241 (1996).

<sup>7</sup>A. Navaza, G. Chevrier, P. Schweiss, and G. Rigotti, J. Solid State Chem. **99**, 158 (1992).

<sup>8</sup>C. Retzlaff, W. Krumbe, M. Dörffel, and S. Haussühl, Z. Kristallogr. **189**, 141 (1989).

<sup>9</sup>P. Klüfers and S. Haussühl, Z. Kristallogr. **170**, 289 (1985).

<sup>10</sup>H. Kogelnik, Bell Syst. Tech. J. **48**, 2909 (1969).

<sup>11</sup>F. Kahmann, J. Opt. Soc. Am. A **10**, 1562 (1993).

<sup>12</sup>G. Borrmann, Phys. Z. **42**, 157 (1941).